Synthesis and Characterization of $A_3Na_{10}Sn_{23}$ (A = Cs, Rb, K) with a New Clathrate-Like Structure and of the Chiral Clathrate $Rb_5Na_3Sn_{25}$

Svilen Bobev and Slavi C. Sevov*

Department of Chemistry and Biochemistry, University of Notre Dame, Notre Dame, Indiana 46556

Received July 13, 2000

Four new compounds $Cs_{17.4(1)}Na_{60.6(1)}Sn_{138}$ (**1**), $Rb_{19.1(1)}Na_{58.9(1)}Sn_{138}$ (**2**), $K_{21.3(1)}Na_{56.7(1)}Sn_{138}$ (**3**), and $Rb_{20}Na_{12}Sn_{100}$ (**4**) were synthesized by fusion of the corresponding elements. The structures were determined by single-crystal X-ray diffraction. Compounds **1**−**3** are isostructural and crystallize in a new structure type (rhombohedral, $R\bar{3}m$, $Z = 1$, $a = 12.4567(9)$ Å, $c = 51.533(3)$ Å for **1**; $a = 12.465(1)$ Å, $c = 51.085(3)$ Å for **2**; $a = 12.456(2)$ Å, $c = 50.559(4)$ Å for **3**). The structure contains layers of fused pentagonal dodecahedra of tin that alternate with layers of isolated tin tetrahedra. It is an intergrowth between the structure of clathrate-II ($A_{24}Sn_{136}$) with the same layers of pentagonal dodecahedra and the Zintl phase ASn with Sn_4^{4-} tetrahedra. Compound **4** is a new chiral clathrate (cubic, $P4_132$, $Z = 1$; $a = 16.4127(7)$ Å) with stoichiometry that corresponds to an electronically balanced Zintl phase.

Introduction

Intermetallic compounds with open frameworks made of tetrels (tetrel = group 14 element) have been known for nearly three and a half decades.[1,2] Over these years they have attracted attention mainly because of their unique structures, but more recently, the interest in these compounds with rigid covalent networks has shifted toward their potential for optical, thermoelectric, and other valuable applications.[3−5] Although theoretical calculations suggest thermodynamic stability for a variety of such frameworks,[6,7] only three structure types have been found so far. They are usually referred to as clathrates, in analogy with the isomorphous gas and liquid hydrates $G_8(H_2O)_{46}$ and $G_8G_{16}(H_2O)_{136}$, respectively (G = Cl_2, Xe, CH_4, CCl_4, etc.).[8] The three clathrates are known as clathrate-I (A_8Tt_{46}), clathrate-II ($A_{24}Tt_{136}$), and chiral clathrate ($A_{32}Tt_{100}$) where A = alkali metal and Tt = tetrel. Clathrate-I crystallizes in the primitive cubic space group $Pm\bar{3}n$ with 46 clathrand atoms per unit cell, all tetrahedrally coordinated by similar atoms. They form 24-atom polyhedra with 12 pentagonal and 2 hexagonal faces called tetrakaidecahedra. These share their hexagonal faces and create a system of three perpendicular and nonintersecting "channels" running along the axes of the cube (Figure 1a). Smaller 20-atom pentagonal dodecahedra are enclosed between the "channels", and their faces are defined by the pentagons of the surrounding tetrakaidecahedra. There are two dodecahedra and six tetrakaidecahedra per cell, and when occupied by cations, the formula of the compound is $A'_2A''_6Tt_{46}$.

Clathrate-II ($A_{24}Tt_{136}$) crystallizes in the face-centered cubic space group $Fd\bar{3}m$. The 136 framework atoms are again four-bonded in a nearly ideal tetrahedral environment and also form two different polyhedra. The key difference is that here the pentagonal dodecahedra are not isolated as in clathrate-I but are rather linked through common faces to form layers. The layers are stacked in ABC sequence as in cubic closest packing, and the second type polyhedra, 28-atoms hexakaidecahedra with 12 pentagonal and 4 hexagonal faces, are enclosed between the layers (Figure 1b). The ratio of smaller to larger cavities in clathrate-II is 16:8, and when occupied by cations, the formula of the clathrate can be written as $A'_{16}A''_8Tt_{136}$.

The chiral clathrate ($A_{32}Tt_{100}$) crystallizes in the rare acentric cubic space group $P4_132$. It contains only pentagonal dodecahedra that share 3 of their 12 pentagonal faces and are also interconnected by exo-bonds. The resulting three-dimensional network can be viewed as made of helical chains of pentagonal dodecahedra along the 4_1 axes (Figure 1c) that are joined together via shared faces and Tt−Tt bonds. An important feature in this structure is that 32 of the 100 clathrand atoms per cell are not four- but rather three-bonded. Thus, its ideal stoichiometry $A_{32}Tt_{100}$ is the only one among the three clathrates that can be rationalized in terms of the Zintl concept as $[A^+]_{32}[(4b\text{-}Tt^0)_{68}(3b\text{-}Tt^{-1})_{32}]$.

The vast majority of the reported binary or pseudobinary A−Tt clathrate compounds adopts type I structure.[9,10] Until recently, only two compounds with the clathrate-II structure were known, the nonstoichiometric Na_xSi_{136} and Na_xGe_{136}.[1,11] The newly added compounds are four stoichiometric mixed-cation Si and Ge clathrates $A_8Na_{16}Tt_{136}$ for A = Cs, Rb and Tt

(1) Kasper, J. S.; Hagenmuller, P.; Pouchard, M.; Cros, C. *Science* **1965**, *150*, 1713.
(2) Gallmeier, J.; Schäfer, H.; Weiss, A. *Z. Naturforsch.* **1969**, *24b*, 665.
(3) Canham, L. T. *Appl. Phys. Lett.* **1990**, *57*, 1046.
(4) Slack, G. A. *Thermoelectric Materials—New Directions and Approaches*; Tritt, T. M., Kanatzidis, M. G., Lyon, H. B. J., Mahan, G. D., Eds.; Materials Research Society: Pittsburgh, PA, 1997; Vol. 478, p 47.
(5) San-Miguel, A.; Keghelian, P.; Blase, X.; Melinon, P.; Perez, A.; Itie, J. P.; Polian, A.; Reny, E.; Cros, C.; Pouchard, M. *Phys. Rev. Lett* **1999**, *83*, 5290.
(6) O'Keeffe, M.; Adams, G. B.; Sankey, O. F. *Philos. Mag. Lett.* **1998**, *78*, 21.
(7) Nesper, R.; Vogel, K.; Blöchl, P. E. *Angew. Chem., Int. Ed. Engl.* **1993**, *32*, 701.
(8) Pauling, L.; Marsh, R. E. *Proc. Acad. Sci. U.S.A.* **1952**, *38*, 112.
(9) *Pearson's Handbook of Crystallographic Data for Intermetallic Phases*; Villars, P., Calvers, L. D., Ed.; ASM International: Materials Park, OH, 1991.
(10) Bobev, S.; Sevov, S. C. *J. Solid State Chem.* **2000**, *153*, 90 and references therein.
(11) Cros, C.; Pouchard, M.; Hagenmuller, P. *J. Solid State Chem.* **1970**, *2*, 570.

10.1021/ic0007714 CCC: $19.00
Published on Web 11/10/2000

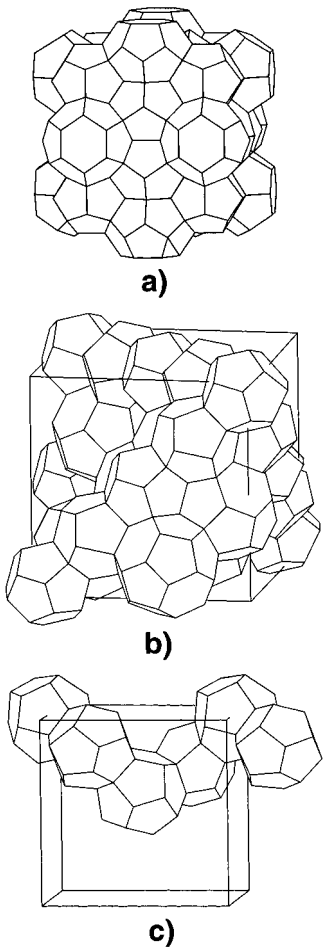

Figure 1. Polyhedral representation of the structures of the three known clathrates: (a) clathrate-I with three perpendicular and nonintersecting chains of tetrakaidecahedra that share hexagonal faces and enclose pentagonal dodecahedra between them; (b) clathrate-II with layers of pentagonal dodecahedra stacked along the body diagonals and enclosing hexakaidecahedra between them; (c) chiral clathrate with only one isolated helical chain of pentagonal dodecahedra shown running along a cubic axis.

= Si, Ge.[10,12] Very few are the compounds with the chiral clathrate structure as well. They are predominantly in the K−Sn and Ba−Ge binary and K−Sn−Bi and Ba−In−Ge ternary systems, some quite nonstoichiometric.[13−16] Clathrate-I and the chiral clathrate can be synthesized in a rational manner with defined compositions and in quantitative yields. The synthesis of clathrate-II compounds, on the other hand, used to be very irreproducible and with low yields and poor homogeneity.[11] Our recent studies of mixed alkali metal systems with silicon and germanium have revealed that cations with very different sizes are crucial for the stabilization of the clathrate-II structure and make the synthesis rational.[10] We have extended these studies to the tin systems, and here we report three new compounds with mixed alkali metals: $Cs_{17.4(1)}Na_{60.6(1)}Sn_{138}$ (**1**), $Rb_{19.1(1)}Na_{58.9(1)}Sn_{138}$ (**2**), and $K_{21.3(1)}Na_{56.7(1)}Sn_{138}$ (**3**) (labeled $A_3Na_{10}Sn_{23}$ hereafter). They crystallize in an unprecedented structure that is an intergrowth between clathrate-II ($A_{24}Sn_{136}$) and the Zintl phase A_4Sn_4. Also, mixed alkali metals in the appropriate ratio stabilize the stoichiometric chiral clathrate $Rb_{20}Na_{12}Sn_{100}$ (**4**), labeled $Rb_5Na_3Sn_{25}$ hereafter.

Experimental Section

Synthesis. All manipulations were performed inside a nitrogen-filled glovebox with controlled oxygen and moisture levels below 1 ppm. The starting materials Na (Alfa, ingot, 99.9% metal basis), K (Alfa, ingot, 99.95% metal basis), Rb (Alfa, sealed under argon, 99.8% metal basis), Cs (Acros, sealed under argon, 99.95%), Sn (Alfa, rod, 99.999% metal basis) were used as received. The surfaces of the Na and K were cleaned with a scalpel immediately before use. Mixtures of the elements were loaded in niobium containers, and the containers were arc-welded under argon. These were subsequently sealed in evacuated fused-silica jackets under a vacuum of ca. 10^{-5} mmHg (below discharge).

The three compounds $A_3Na_{10}Sn_{23}$ were initially identified as products of reactions loaded as $A_8Na_{16}Sn_{136}$ (A = Cs, Rb, K) and intended to produce Sn-based clathrate-II phases analogous to the Si and Ge clathrates $A_8Na_{16}Si_{136}$ and $A_8Na_{16}Ge_{136}$.[10] The mixtures were heated at 400 °C for 3 weeks and then were slowly cooled to room temperature at a rate of 5 °C/h. After the structures were determined from single-crystal X-ray diffraction, the ratio of total alkali metal (A + Na) to tin was clear but the proportions of the two alkali metals were ambiguous because of possible mixing at some cation sites. Elemental analysis with ICP on selected crystals of $Cs_3Na_{10}Sn_{23}$ gave a ratio of ca. 1:3 for Cs/Na (5.87 wt % Na and 14.52 wt % Cs). Series of reactions were loaded with constant (A + Na)/Sn ratio but with A/Na ratios varying from 1:1 to 1:4. Nevertheless, none of these provided pure phases, and the yields were quite low. It was later realized that the tin acts apparently as a flux, and the yields could be increased dramatically when excess of tin was used. Thus, **1** was synthesized nearly as a single phase (and left elemental tin) from reaction loaded as $CsNa_3Sn_{10}$ under the above-mentioned conditions. The reaction loaded as $RbNa_3Sn_{10}$ produced **2** and **4** simultaneously. All attempts to make **2** only were unsuccessful. Compound **4**, on the other hand, was later synthesized without compound **2** (but with extra tin present) as very fine powder by quenching a reaction loaded as $Rb_5Na_3Sn_{40}$. Compound **3** was one of the products of a mixture with stoichiometry KNa_3Sn_{10}, but the yield was also low. The other products of this reaction were NaSn and a phase isostructural with the known $Rb_{12}Si_{17}$ and presumed to be $K_{12}Sn_{17}$.[17] It seems all four compounds are incongruently melting.

The crystals of **1**−**3** are gray but shiny and with metallic luster, while those of **4** are dark-gray and without metallic luster. For all four compounds it was relatively easy to separate the bar-like crystals from the dustlike leftover Sn in order to perform measurements. All four compounds are relatively air-stable, although crystals with crystallographic quality could not be found after the samples were exposed to air and moisture. Nonetheless, powder X-ray diffraction confirmed their stability after 12 h soaking in water.

X-ray Diffraction Studies. The outcome of all reactions was monitored by powder X-ray diffraction using an Enraf-Nonius Guinier camera with Cu $K\alpha_1$ radiation. The diffraction patterns were also used to verify the unit cell parameters by least-squares refinements of the positions of the lines, calibrated by silicon (NIST) as an internal standard. The lattice parameters of **1**−**3** from reactions loaded with different A/Na ratios changed only within 6.5σ, an indication of line compounds or compounds with very narrow phase width.

For the single-crystal studies a few crystals from each compound were selected, mounted in 0.2 mm Lindemann glass capillaries (subsequently sealed at both ends), and checked for singularity. For the best ones, diffraction data were collected on an Enraf-Nonius CAD-4 diffractometer with graphite monochromated Mo Kα radiation ($\omega-2\theta$ scans) at room temperature. The crystals of **1** were of very good quality, while the crystals of **2** and especially of **3** were considerably worse. Quadrants of data were collected from crystals of **1** (0.18 mm × 0.16 mm × 0.10 mm, $2\theta_{max} = 60°$), **2** (0.14 × 0.10 × 0.08 mm, $2\theta_{max} = 50°$), and **3** (0.10 mm × 0.08 mm × 0.06 mm, $2\theta_{max} = 60°$), and an

(12) Bobev, S.; Sevov, S. C. *J. Am. Chem. Soc.* **1999**, *121*, 3795.
(13) Zhao, J.-T.; Corbett, J. D. *Inorg. Chem.* **1994**, *33*, 2343.
(14) von Schnering, H.-G.; Kröner, R.; Carrilo-Cabrera, W.; Peters, K.; Nesper, R. *Z. Kristallogr.—New Cryst. Struct.* **1998**, *213*, 665.
(15) Fässler, T. F.; Kronseder, C. *Z. Anorg. Allg. Chem.* **1998**, *624*, 561.
(16) Fukuoka, H.; Iwai, K.; Yamanaka, S.; Abe, H.; Yoza, K.; Häming, L. *J. Solid State Chem.* **2000**, *151*, 117.
(17) Queneau, V.; Todorov, E.; Sevov, S. C. *J. Am. Chem. Soc.* **1998**, *120*, 3263.

Table 1. Selected Details of the Structural Studies for $A_3Na_{10}Sn_{23}$ (A = Cs, Rb, K) and $Rb_5Na_3Sn_{25}$

chemical formula	$Cs_{17.4(1)}Na_{60.6(1)}Sn_{138}$	$Rb_{19.1(1)}Na_{58.9(1)}Sn_{138}$	$K_{21.3(1)}Na_{56.7(1)}Sn_{138}$	$Rb_{20}Na_{12}Sn_{100}$
space group, No.	$R\bar{3}m$, 166	$R\bar{3}m$, 166	$R\bar{3}m$, 166	$P4_132$, 213
fw	20085.05	19363.93	18515.58	13854.28
temp (°C)		21(2)		
radiation, λ (Å)		Mo Kα, 0.710 73		
a (Å)	12.4567(9)	12.465(1)	12.456(2)	16.4127(7)
c (Å)	51.533(3)	51.085(3)	50.559(4)	
V (Å^3), Z	6925.0(8), 1	6874.4(9), 1	6793.9(9), 1	4421.2(3), 1
ρ_{calc} (g/cm^3)	4.816	4.677	4.526	5.203
μ (cm^{-1})	145.34	157.22	128.37	193.25
R1/wR2 [a] (%), $I > 2\sigma_I$	3.64/8.64	3.61/7.95	6.67/13.80	2.71/6.12
R1/wR2 (%), all data	4.41/8.81	4.78/8.73	12.63/16.12	3.24/6.27

[a] $R1 = [\sum||F_o| - |F_c||]/\sum|F_o|$; $wR2 = \{[\sum w[(F_o)^2 - (F_c)^2]^2]/[\sum w(F_o^2)^2]\}^{1/2}$; $w = [\sigma^2(F_o)^2 + (AP)^2 + BP]^{-1}$, where $P = [(F_o)^2 + 2(F_c)^2]/3$.

Table 2. Atomic Coordinates and Equivalent Isotropic Displacement Parameters (U_{eq})[a] for $Cs_3Na_{10}Sn_{23}$ and $Rb_5Na_3Sn_{25}$

atom	site	x	y	z	U_{eq} (Å^2)	occup
			$Cs_3Na_{10}Sn_{23}$			
Sn1	*6c*	0	0	0.13874(2)	0.0169(2)	1.0
Sn2	*6c*	0	0	0.19472(2)	0.0171(2)	1.0
Sn3	*18h*	0.20009(3)	$-x$	0.16667(1)	0.0148(1)	1.0
Sn4	*18h*	0.12471(3)	$-x$	0.12020(1)	0.0161(1)	1.0
Sn5	*36i*	0.33299(4)	0.28405(4)	0.089501(9)	0.0177(1)	1.0
Sn6	*18h*	0.12461(3)	$-x$	0.21314(1)	0.0162(1)	1.0
Sn7	*6c*	0	0	0.37393(3)	0.0476(4)	1.0
Sn8	*18h*	0.07867(9)	$-x$	0.32821(3)	0.0933(7)	0.9(1)
Sn9	*18h*	0.075(1)	$-x$	0.6717(3)	0.0933(7)	0.1(1)
Sn10	*18h*	0.0770(1)	$-x$	0.00107(6)	0.0599(6)	0.5
Sn11	*6c*	0	0	0.04561(9)	0.056(1)	0.5
Cs1	*9d*	$^1/_2$	0	$^1/_2$	0.0197(2)	1.0
Cs2	*6c*	0	0	0.44546(3)	0.0611(5)	1.0
Na1	*18h*	0.4876(4)	$-x$	0.0507(1)	0.059(2)	1.0
Na2	*18h*	0.1680(5)	$-x$	0.0440(2)	0.094(3)	1.0
Cs/Na3[b]	*6c*	0	0	0.06855(7)	0.026(1)	0.5
Cs/Na4[c]	*6c*	0	0	0.2644(1)	0.054(2)	1.0
Na5	*18h*	0.1571(8)	$-x$	$-0.0315(4)$	0.058(4)	0.5
Na51	*18h*	0.1865(8)	$-x$	$-0.0342(4)$	0.068(5)	0.5
			$Rb_5Na_3Sn_{25}$			
Sn1	*8c*	0.03431(4)	x	x	0.0210(3)	1.0
Sn2	*24e*	0.20503(4)	0.04408(5)	0.00134(4)	0.0175(2)	1.0
Sn3	*12d*	1/8	0.16808(5)	$^1/_4 + y$	0.0189(2)	1.0
Sn4	*24e*	0.23963(4)	0.93368(5)	0.87370(5)	0.0180(2)	1.0
Sn5	*24e*	0.41655(5)	0.85075(5)	0.08694(5)	0.0221(2)	1.0
Sn6	*8c*	0.32489(4)	x	x	0.0194(3)	1.0
Rb1	*8c*	0.18962(7)	x	x	0.0254(4)	1.0
Rb2	*24e*	0.4393(3)	0.8234(4)	0.3062(3)	0.126(3)	0.5
Na3	*24e*	0.4115(8)	0.726(1)	0.226(1)	0.24(2)	0.5

[a] U_{eq} is defined as one-third of the trace of the orthogonalized U_{ij} tensor [b] Cs/Na3 = $Cs_{0.5(1)}Na_{0.5(1)}$. [c] Cs/Na4 = $Cs_{0.15(2)}Na_{0.85(2)}$.

octant of data was collected for **4** (0.14 mm × 0.10 mm × 0.08 mm, $2\theta_{max} = 50°$). The data sets were corrected for absorption using the average of five ψ scans for **1**, **2**, and **4** and two ψ scans for **3**. The four structures were solved and refined on F^2 with the aid of the SHELXTL, version 5.1, software package. Important crystallographic parameters and details for the refinements of the four compounds are summarized in Table 1. The final positional and equivalent isotropic displacement parameters for **1** and **4** are listed in Table 2, while important distances for the two compounds are given in Tables 3 and 4, respectively. Tables for the Rb and K analogues of $Cs_3Na_{10}Sn_{23}$ are given as Supporting Information.

Magnetic Measurements. These were carried out on a Quantum Design MPMS superconducting quantum interference device (SQUID) magnetometer at a field of 3 T over the temperature range 10−290 K. The samples were contained in special holders designed for air-sensitive compounds (details can be found elsewhere).[18] The magnetization of a 57 mg sample of **1** made only of crystals carefully picked under microscope was corrected for the holder and for the ion-core diamagnetism as well as for Larmor precession of the delocalized electrons. The resulting temperature-independent magnetic susceptibility is within the range 2.44×10^{-4} to 2.79×10^{-4} emu/mol and indicates metallic Pauli-like paramagnetism. The metallic behavior was confirmed by a qualitative two-probe conductivity test on a single crystal of the same sample. Since complete separation of **2** and **4** was not possible, the susceptibility of **2** could not be established accurately. Nevertheless, the SQUID signal of 48 mg of a mixture of **2** and **4** was flat, and the raw magnetization at room temperature was negative, -2.7×10^{-4} emu. The raw magnetization of 63 mg of **3** (also not pure) was also temperature-independent and also negative, -7×10^{-4} emu. The molar susceptibility of 71 mg of pure **4** was negative in the range $-(1.34-1.40) \times 10^{-3}$ emu/mol, clearly indicating diamagnetic behavior of the electronically balanced Zintl phase $Rb_5Na_3Sn_{25}$. This, combined with the result for the mixture of **2** and **4** (above), suggests that the molar susceptibility of **2** is perhaps positive after the appropriate corrections are applied.

Structure Determination. The routine indexing and cell reduction unambiguously indicated rhombohedral cells for $A_3Na_{10}Sn_{23}$, and the structures were solved successfully in $R\bar{3}m$. Direct methods provided all Sn positions and the positions of the heavier cations. The remaining cations were later identified from difference Fourier maps. The distances between equivalent tin atoms of one position, Sn10, as well as the distances between a cation position and another tin site, Sn11, were unreasonably short, and this, combined with large thermal parameters for these positions, clearly suggested fractional occupancies. When freed to vary, the occupancies deviated significantly from full and were rather close to a half, and they were later refined as fixed at 50%. Short distances were also encountered between two other tin sites, Sn8 and Sn9. Their occupancies were refined as close to 90 and 10%, respectively, and therefore, they were refined to add up to 100%.

In addition to these, the distances around two cation sites were too long for sodium but too short for cesium. Similarly, the coordination numbers were too high for Na but too low for Cs. Therefore, these two positions, Cs/Na3 and Cs/Na4, were refined as mixed. The different A/Na ratios in the three compounds $A_3Na_{10}Sn_{23}$ lead to somewhat different formulas for them, $Cs_{2.90(2)}Na_{10.10(2)}Sn_{23}$, $Rb_{3.18(2)}Na_{9.82(2)}Sn_{23}$ and $K_{3.55(2)}Na_{9.45(2)}Sn_{23}$. A third cation site occupied by sodium was refined with unusually elongated and large thermal ellipsoid. It had a somewhat short distance to a half-occupied tin atom, Sn10, which suggested fractional occupancy. The occupancy factor was free to vary but did not deviate by more than 5σ from unity. This, in turn, suggested two half-occupied positions, Na5 and Na51, along the elongated axis of the ellipsoid. This led to much better thermal parameters and also solved the distance problem.

It should be pointed out that extensive efforts were made to refine the structure in the acentric $R3m$ in order to (hopefully) avoid the above-mentioned problems. There are a few indications that the acentric space group may be the better choice. These include the short distances between inversion center-generated equivalent positions of Sn10, between Sn11 and Cs/Na3, the need to split one sodium position between Na5 and Na51, and the need to refine all of these half-occupied. The refinement with well-behaved atoms only gave similar residual factors as when refined in the centric space group. Nevertheless, the subsequent difference Fourier map indicated remaining electron density at exactly the same positions as in $R\bar{3}m$. Thus, two pairs of different tin atoms replaced Sn10 and Sn11, and a pair of mixed cations replaced

(18) Bobev, S.; Sevov, S. C. *Inorg. Chem.* **1999**, *38*, 1805.

Table 3. Important Distances (Å) in $Cs_3Na_{10}Sn_{23}$

bond			bond			bond		
Sn1−	3Sn4	2.8852(7)	Sn9−	2Sn9	2.82(5)	Na2−	Sn10	2.96(1)
	Sn2	2.885(2)		Sn7	2.88(2)		Sn9	3.20(3)
	Cs/Na3	3.617(4)		Na2	3.20(3)		2Sn5	3.387(7)
	3Cs1	3.8732(5)		Cs/Na4	3.65(2)		2Na1	3.472(7)
Sn2−	3Sn6	2.8511(7)		4Na1	4.09(1)		2Na5	3.57(1)
	Sn1	2.885(2)	Sn10−	Sn11	2.834(5)		2Na51	3.87(2)
	Cs/Na4	3.590(6)		Sn11	2.924(5)		Sn7	3.57(1)
	3Cs1	3.8757(5)		2Sn10	2.879(4)		Sn11	3.63(1)
Sn3−	2Sn3	2.8748(6)		Na2	2.96(1)		Cs/Na3	3.84(1)
	Sn4	2.8948(9)		Na51	2.98(2)		Na5	3.90(2)
	Sn6	2.8960(9)		2Na5	3.33(1)		Na51	4.05(2)
	2Cs1	4.0054(5)		Cs/Na3	3.854(4)		2Sn10	3.91(1)
	2Cs2	4.020(1)		2Na2	3.91(1)		2Sn8	3.995(9)
Sn4−	Sn1	2.8852(7)	Sn11−	3Sn10	2.834(5)	Cs/Na3−	Sn1	3.617(4)
	2Sn5	2.8812(6)		3Sn10	2.924(5)		3Sn4	3.785(3)
	Sn3	2.8948(9)		3Na5	3.47(2)		3Na2	3.84(1)
	Cs/Na3	3.785(3)		3Na51	4.07(2)		3Sn10	3.854(4)
	2Cs1	4.0284(4)		3Na2	3.63(1)		3Na5	3.89(2)
	Cs2	4.5204(7)	Cs1−	2Sn1	3.8732(5)		3Na51	4.40(2)
Sn5−	Sn4	2.8812(6)		2Sn2	3.8757(5)		6Sn5	4.027(1)
	Sn6	2.8871(6)		4Sn3	4.0054(5)	Cs/Na4−	Sn2	3.590(6)
	Sn5	2.9287(9)		4Sn4	4.0284(4)		3Na51	3.64(2)
	Na1	3.213(5)		4Sn6	4.0283(5)		3Na5	4.26(1)
	Na51	3.23(2)		4Sn5	4.2376(5)		3Sn9	3.65(2)
	Na5	3.33(2)	Cs2−	Sn7	3.686(2)		3Sn8	3.701(5)
	Na2	3.387(7)		6Sn3	4.020(1)		3Sn6	3.769(4)
	Cs/Na3	4.027(1)		3Sn4	4.5204(7)		3Na1	3.976(8)
	Cs/Na4	4.028(2)		3Sn6	4.5225(7)		6Sn5	4.028(2)
	Cs1	4.2376(5)		3Na1	4.595(8)	Na5−	2Sn10	3.33(1)
	Cs2	4.9046(7)		6Sn5	4.9046(7)		2Sn5	3.33(2)
Sn6−	Sn2	2.8511(7)		3Na2	5.01(1)		Sn11	3.47(2)
	2Sn5	2.8871(6)	Na1−	Sn8	3.193(8)		2Sn8	3.57(2)
	Sn3	2.8960(9)		2Sn5	3.213(5)		2Na2	3.57(1)
	Cs/Na4	3.769(4)		Sn8	3.306(7)		Cs/Na3	3.89(2)
	Na1	3.770(7)		Sn7	3.369(8)		Na2	3.90(2)
	2Cs1	4.0283(5)		2Na2	3.472(7)		2Na1	3.958(9)
	Cs2	4.5225(7)		2Na51	3.665(9)		Cs/Na4	4.26(1)
Sn7−	3Sn8	2.904(2)		2Na5	3.958(9)	Na51−	Sn10	2.98(2)
	3Sn9	2.88(2)		Sn6	3.770(7)		2Sn8	3.13(2)
	3Na1	3.369(8)		Cs/Na4	3.976(8)		2Sn5	3.23(2)
	3Na2	3.57(1)		2Sn9	4.09(1)		Cs/Na4	3.64(2)
	Cs2	3.686(2)		Cs2	4.595(8)		2Na1	3.665(9)
Sn8−	Sn7	2.904(2)					2Na2	3.87(2)
	2Sn8	2.940(3)					Sn11	4.07(2)
	2Na51	3.87(2)					Na2	4.05(2)
	2Na5	3.57(2)					Cs/Na3	4.40(2)
	Na1	3.193(8)						
	Na1	3.306(7)						
	Cs/Na4	3.701(5)						
	2Na2	3.995(9)						

the Cs/Na3 position. When refined independently, the occupancy factors for all converged to 50% within a few standard deviations. The final *R* factors were virtually the same as those from the refinement in $R\bar{3}m$. This indicates that the disorder in these sites is truly statistical because of the equivalent environment around the "different" positions in *R*3*m*, which in turn is due to the "centricity" of the rest of the structure. This is quite a common refinement problem for structures with a major centric part and a small acentric fraction.

The X-ray data collected from the crystal of **4** readily indicated the only two possible enantiomorphic cubic space groups $P4_132$ and $P4_3$-32. The structure was successfully solved in the former, and the direct methods provided all six Sn and two Rb sites. One of the latter, Rb1 (*8c*), centers a pentagonal dodecahedron of tin while the other one, Rb2 (*24e*), is very close to a 2-fold axis and therefore becomes unreasonably close to its symmetry equivalent. This indicated that the position could not be occupied more than 50%, and it was refined as half-occupied. A third cation position, Na3 (*24e*), was found from the difference Fourier map. It is too close to the Rb2 position but at good distance to its equivalent generated by the 2-fold axis. It was also refined as half-occupied, and thus, Rb2 and Na3 account for one full alkali metal cation.

Results and Discussion

$Cs_3Na_{10}Sn_{23}$. Since the three compounds $A_3Na_{10}Sn_{23}$ for A = K, Rb, and Cs are isostructural, we will discuss in detail only $Cs_3Na_{10}Sn_{23}$. The structure consists of layers made of fused pentagonal dodecahedra of tin that alternate with layers of isolated tin tetrahedra and cations (Figure 2). It is an intergrowth of two structures that contain these building blocks separately, the layers of pentagonal dodecahedra of clathrate-II (Figure 3) and the isolated Sn_4 tetrahedra of the Zintl phase ASn (=A_4Sn_4). The stacking order of the dodecahedral layers in both clathrate-II ($Fd\bar{3}m$) and the rhombohedral cell of $A_3Na_{10}Sn_{23}$ (=$A_6Na_{20}Sn_{46}$) is the same, cubic ABC (Figures 2 and 3). Of course, in the clathrate such stacking occurs along all four body diagonals of the cubic cell. Thus, the structure of $A_3Na_{10}Sn_{23}$ can be viewed as an intercalation compound of clathrate-II (A_6Sn_{34}) intercalated with three Sn_4^{4-} tetrahedra and 20 Na atoms per layer, i.e., $A_6Na_{20}Sn_{46} = A_6Sn_{34} + 20Na + 3Sn_4$, which can be also represented as 12 mol of the Zintl phase NaSn and

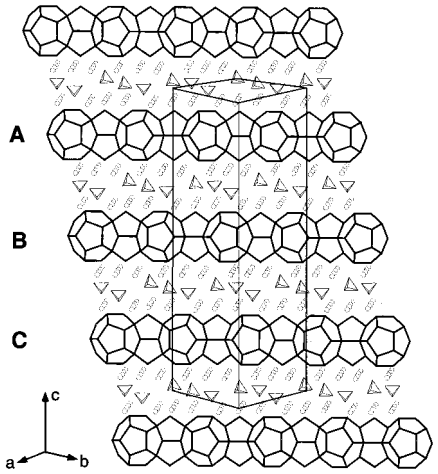

Figure 2. General view of the structure of $Cs_3Na_{10}Sn_{23}$ (rhombohedral, *R*3*m*, the unit cell is outlined). Layers of tin dodecahedra are stacked in ABC order along the *c* axis. The interlayer spacing is filled with layers of isolated tin tetrahedra and alkali metal cations (open circles). The cations residing within the clathrate layers are omitted for clarity.

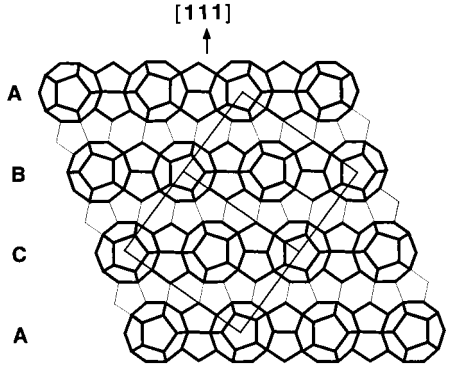

Figure 3. Structure of clathrate-II shown in a projection perpendicular to a body diagonal of the cubic cell. The layers of fused dodecahedra and the unit cell are outlined. The larger hexakaidecahedra can be seen between the layers.

8 extra Na atoms, i.e., $A_6Na_{20}Sn_{46} = A_6Sn_{34} + 12NaSn + 8Na$. Six of the eight extra electrons provided by the extra alkali metal atoms act as "electronic scissors" and "cut" the Sn−Sn bonds between the layers of dodecahedra in clathrate-II to open space for the rest of the intercalating material. This process of reduction and breakage of bonds creates twelve 3-bonded tin atoms (all are 4-bonded in the clathrate) on the surface of the layers. These atoms take the extra electrons to become Sn^- with lone pairs of electrons, and the layer becomes $Sn_{34}{}^{12-}$. This is the inverse of the recently described "zipping" oxidation of $A_2Bi_4Se_7$ to ABi_2Se_7 where bonds between layers are formed upon removal of cations,[19] and therefore, it can be analogously called "unzipping" reduction. The remaining two extra electrons of the extra alkali metal atoms become delocalized over the whole structure and make the compound metallic. Indeed, the metallic luster and the appearance of the crystals, the qualitative two-probe conductivity tests, and more importantly the measured weak and temperature-independent Pauli paramagnetism all indicate metallic properties. The formula of the layered clathrate, therefore, should be rewritten as follows:

$$A_6Na_{20}Sn_{46} = \{[A_6(Sn_{34}{}^{12-})]^{6-} + 6Na^+\} + 3(Na_4Sn_4)^0 + [2Na^+ + 2e^- (\text{delocalized})]$$

A more detailed description of the building elements of the structure follows. The dodecahedra of the layers are made of six crystallographically distinct Sn atoms, Sn1 to Sn6. They are centrosymmetric with a slight deviation from the ideal icosahedral I_h point-group symmetry. Each dodecahedron shares two sets of parallel faces with four other dodecahedra. The layers are honeycombs of six-membered rings of such face-sharing dodecahedra (Figure 4). The Sn−Sn distances in the layer, from 2.8511(7) to 2.9287(9) Å, are somewhat longer than the distances in the semiconducting α-Sn, 2.810 Å, the electron-deficient $K_{7.4}Sn_{25}$, 2.82−2.86 Å,[13] and the electronically balanced Zintl phases $A_8Sn_{44}\square_2$, 2.70−2.88 Å.[10,13] This elongaition is a result of the two extra electrons per clathrate layer, which presumably populate the conduction, antibonding band of the layer and cause the bond weakening. A similar effect is seen in the electron-richer clathrate-II compounds of Si and Ge.[10,12]

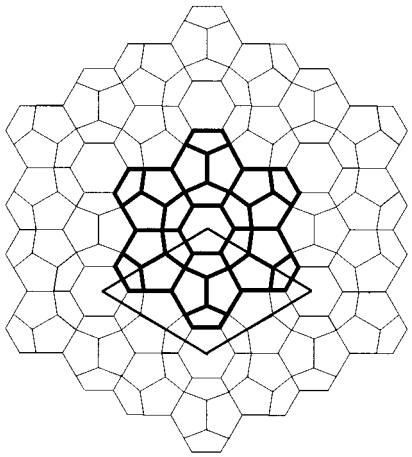

Figure 4. View normal to the honeycomb layer of hexagons of fused dodecahedra of tin. Outlined is one such hexagon of six dodecahedra.

All four-bonded tin atoms, Sn1−Sn4 and Sn6, are surrounded by four cesium or mixed alkali metal cations (Table 3), while more cations, six, are "attracted" by the lone pair of electrons of the three-bonded tin atom, Sn5. The last is the only tin atom from the layer that is exposed to sodium cations and with relatively short Na−Sn distances.

The second building motif in the structure is the $Sn_4{}^{4-}$ tetrahedra arranged in layers that are positioned at $z \approx 0$, $^1/_3$, and $^2/_3$ between the dodecahedral layers. Such tetrahedra also exist in the Zintl phases ASn (=A_4Sn_4)[20,21] where they are the only species. Their coexistence with layers of clathrate-II in $A_3Na_{10}Sn_{23}$ makes the latter an intermediate in a structural "conversion" of A_4Tt_4 to the clathrate-II $A'_2A''_4Tt_{34}$. The tetrahedra are very disordered in $A_3Na_{10}Sn_{23}$ most likely because of mismatch in packing with the layers. There are five tin sites that participate in the formation of two crystallographically distinct tetrahedra labeled **A** (Sn7, Sn8, Sn9) and **B** (Sn10, Sn11). Tetrahedron **A** has two orientations defined by two staggered triangular bases made of three Sn8 and three Sn9 atoms and a common vertex of Sn7 (Figure 5a). A 3-fold axis passes through Sn7 and the center of the triangular base. Sn7 was refined with full occupancy, an indication that the tetrahedron itself is also fully occupied but with two different orientations. Thus, the occupancies of Sn8 and Sn9 were free to be refined but constrained to add to 100%. The refinement showed a Sn8/Sn9 ratio of 9:1. The Sn9 position is clearly less preferred most likely because of the uncomfortable distances

(19) Iordanidis, L.; Kanatzidis, M. G. *Angew. Chem., Int. Ed. Engl.* **2000**, *39*, 1927.
(20) Müller, W.; Volk, K. *Z. Naturforsch.* **1977**, *32b*, 709.
(21) Hewaidy, I. F.; Busmann, E.; Klemm, W. *Z. Anorg. Allg. Chem.* **1964**, *328*, 283.

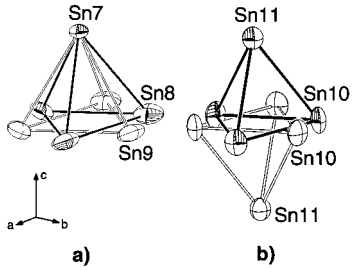

Figure 5. Shown are the isolated tetrahedra of tin: (a) the two orientations of tetrahedron **A** made of three Sn8 and one Sn7 atoms or three Sn9 and one Sn7 atoms; (b) the two orientations of tetrahedron **B** made of three Sn10 and one Sn11 atoms related by inversion center. The thermal ellipsoids are drawn at the 50% probability level.

associated with it. Thus, while Sn8−Sn8 and Sn8−Sn7 distances are 2.940(3) and 2.904(2) Å, respectively, the corresponding Sn9−Sn9 and Sn9−Sn7 distances are 2.82(5) and 2.88(2) Å, respectively. The electron density at the Sn9 site is very low and very diffuse, the "location" of the atom is very uncertain, and as a result, the distances have very large deviations. These short distances are forced by the even closer contacts with nearby cation sites, Na2, Na5, and Cs/Na4 (Table 3).

Tetrahedron **B** is made of half-occupied positions, a triangle of Sn10 and an apex of Sn11. It has two equivalent positions related by an inversion center. Sn11 is on a 3-fold axis while two sets of three Sn10 atoms form two staggered triangular bases (Figure 5b). Each triangle is combined with a Sn11 atom, one "up" and one "down" as shown in Figure 5b. In other words, in half of the unit cells the tetrahedron points up and the in other half it points down. The Sn10−Sn10 and Sn10−Sn11 distances are 2.879(4) and 2.924(5) Å, respectively. Alternating with the Sn11 vertex is a nearby Cs/Na3 mixed alkali metal position that is also half-occupied. Thus, when the tetrahedron points "up", the alkali metal is below the triangular base, and when it points "down", the cation is above the base (Figure 6c,d).

Figure 6 shows the coordination of cations around the two tetrahedra. Three Na1 and three Na5 atoms bridge the edges, three Na2 and one Cs/Na4 cap the faces, and other three Na1 are exo-atoms to the Sn8 vertexes of the tetrahedron made of Sn7 and Sn8 (Figure 6a). The staggered orientation of this tetrahedron, which exists only 10% of the time, is made of Sn7 and Sn9, and most of the surrounding cations switch roles. Thus, the edges in this orientation are bridged by three Na2 and three Na1 atoms, the faces are capped by three Na1 and one Cs/Na4, and exo-atoms to Sn9 are three Na5 cations (Figure 6b). Very similar cation distribution is found around tetrahedron **B**. Three Na2 and one Cs/Na3 cap the faces, three Na5 bridge the three Sn10−Sn10 edges, and three pairs of Na51 and Na2 are exo-atoms to the three Sn10 vertexes in the "up" position of the tetrahedron (Figure 6c). In its "down" position (Figure 6d) the base is rotated by 60° and the Sn11 vertex occupies the down position but the roles of the cations remain the same except that the atoms above and below the plane of the base of Sn10 atoms switch roles.

The number of cations and the refined A/Na ratios need to be discussed in some more detail. Two of the eight cation sites are clearly occupied by the heavy alkali metal A. These are Cs1 inside the pentagonal dodecahedra of the layers (CN = 20) and Cs2 located above and below the centers of the hexagonal rings formed by the dodecahedra (Figure 7). The latter positions are near the centers of incomplete tin hexakaidecahedra with only 18 of the total of 28 vertexes needed for its

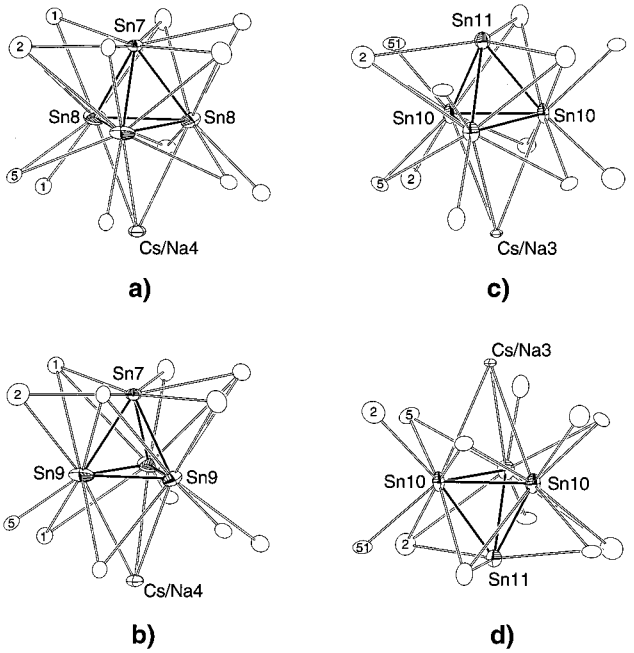

Figure 6. Alkali metal coordination around the two orientations of tetrahedron **A** (a, b) and the two orientations of tetrahedron **B** (c, d). The tin atoms are shown as full thermal ellipsoids, the Na atoms are shown as open (enumerated) circles, and the mixed Cs/Na4 and Cs/Na3 sites are represented with crossed circles. All thermal ellipsoids are drawn at the 30% probability level.

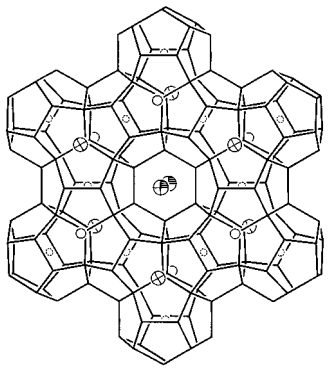

Figure 7. One hexagon of the layer of fused dodecahedra and the surrounding cations, the latter shown as isolated atoms. Cs1 (dotted circles) are inside the dodecahedra, Cs2 (full ellipsoids) are above and below the central hexagon, and Cs/Na3 (open circles) and Cs/Na4 (crossed circles) alternate in the smaller crevices above and below the layer.

completion. These 18 atoms form a "cup" with a hexagonal base and six pentagonal sides. Two cups are fused along the bottoms and open up away from the layer (Figure 7). Cs2 centers the cup but is shifted from the center of the imaginary completed hexacaidecahedron toward the hexagonal bottom of the cup. This makes "normal" the Cs distances to the six Sn3 atoms of that hexagon, 4.020(1) Å, which would have been too long, ca. 4.65 Å, had the cesium been at the hexacaidecahedron's center. The distances to the remaining atoms of the cup (three Sn4 at 4.5204(7) Å, three Sn6 at 4.5225(7) Å, and six Sn5 at 4.9046-(7) Å) remain quite long because the shift of Cs2 from the center is either lateral to them or away from them. It is appropriate here to discuss in a wider context the distances in an imaginary complete hexakaidecahedron of tin to its center. Because of the tin size and the resulting Sn−Sn distances, the cage becomes so large that the distances to the center become too long (estimated radius of ca. 5 Å) for even the largest cation in the

periodic table, Cs, to fit comfortably. As we have discussed it elsewhere,[10] this is the most likely reason for the nonexistence of clathrate-II structures based on Sn. Simply, there are no large enough cations to fit in the hexakaidecahedra of the tin-based clathrate-II structure. Cesium and rubidium fit well in the much smaller hexakaidecahedra of silicon and germanium and stabilize the clathrate-II compounds $Cs_8Na_{16}Si_{136}$, $Cs_8Na_{16}Ge_{136}$, $Rb_8Na_{16}Si_{136}$, $Rb_8Na_{16}Ge_{136}$.[10,12] Also, since clathrate-I is built of the smaller tetrakaidecahedra in addition to the dodecahedra, it could and does exist with potassium, rubidium, and cesium but not with the too small sodium where structures with "collapsed" channels seem to be predominant.[22,23] Similarly, the chiral clathrate with only dodecahedra should exist with these three cations as well, although the only tin-based compounds known prior to this work were with potassium, i.e., K_xSn_{25} for $x = 7.4$ and 6. Thus, the incomplete cage in $Cs_3Na_{10}Sn_{23}$ and the shift of Cs2 from the center is the "answer" to the problem of the oversized cage. Furthermore, Cs2 has another tin neighbor, Sn7 from tetrahedron **A**, which is positioned opposite the hexagonal face of six Sn3 atoms and is also quite close to the cesium, 3.686(2) Å. The coordination is completed by six sodium atoms, giving a total coordination number of 25 for Cs2. As a result of the large coordination number and oversized cage, the thermal parameter of Cs2 is larger than that of Cs1. The situation in the case of $K_3Na_{10}Sn_{23}$ is the worst because the corresponding potassium cation at this site is even smaller and apparently "rattles" in the cage so that the electron density at the position becomes extremely smeared along the direction of the 3-fold axis, and a relatively high residual electron density remains there in the final refinement.

Two cation positions labeled Cs/Na3 and Cs/Na4 are refined as mixed alkali metals. The reasons are that (i) the distances around them are too long for sodium and too short for cesium (Table 3), (ii) their coordination numbers are lower than those of Cs1 and Cs2 but are higher than the coordination numbers of the sodium sites (Table 3), and (iii) the electron density at these sites is quite diffused, which is usually an indication of disorder. Position Cs/Na3 caps the triangle made of three Sn10 atoms in tetrahedron **B**, while Cs/Na4 does the same for the triangle of either atom Sn8 or Sn9 in tetrahedron **A** (Figure 6). While the Cs cations are involved primarily in interactions within the clathrate layer, the Na cations are involved in interactions only within the layer of tetrahedra, keeping the tetrahedra apart and screening their negative charges. Interestingly, the mixed Cs/Na sites are positioned between the clathrate layer of tetrahedra, i.e., an intermediate positioning. Position Cs/Na3 has almost equal participation of Cs and Na but is half-occupied because it alternates with Sn11 (Figure 6), while Cs/Na4 was refined as $Cs_{0.15(2)}Na_{0.85(2)}$. The variations of the fractions in these two mixed positions define any stoichiometry width that might be there for these compounds and also give somewhat different A/Na ratios for A = Cs, Rb, or K, i.e., $Cs_{17.4(1)}Na_{60.6(1)}Sn_{138}$, $Rb_{19.1(1)}Na_{58.9(1)}Sn_{138}$, and $K_{21.3(1)}Na_{56.7(1)}Sn_{138}$.

Na5 and Na51 need special attention. They were initially refined as a single sodium position. This resulted in a thermal ellipsoid that was very elongated radially from tetrahedron **B** and was also too close to the half-occupied Sn10 position. The problem was solved by splitting the position to two half-occupied sites, Na5 and Na51, along the long axis of the ellipsoid. Thus, Na51 is further removed from the tetrahedron and is an exo-atom to Sn10 at a short, but not without precedent, distance of 2.98(2) Å.[23−25] The other half of this position, Na5, bridges the Sn10−Sn10 edges of the tetrahedron at 3.33(1) Å.

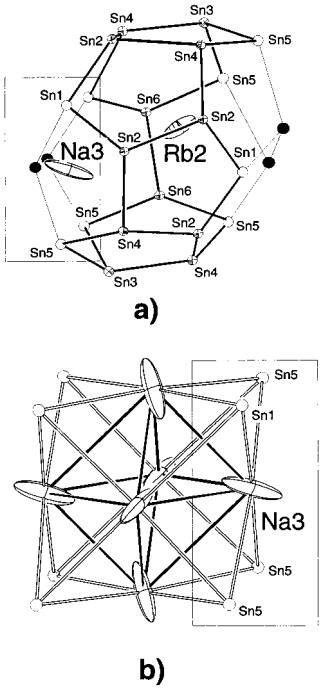

Figure 8. Shown are (a) the incomplete polyhedron around the half-occupied positions Rb2 and Na3 and (b) the equivalent positions of Na3 around the center of a cavity formed by the three-bonded Sn atoms (open circles) in the chiral clathrate $Rb_5Na_3Sn_{25}$. (a) The imaginary polyhedron is made of Sn2, Sn3, Sn4, and Sn6 (full ellipsoids), Sn1 and Sn5 (open circles), and imaginary atoms (black circles). All thermal ellipsoids are drawn at the 20% probability level.

The overall composition of $Cs_3Na_{10}Sn_{23}$ or $A_{13}Sn_{23}$ ($=A_{16}Sn_{28.31}$) where A is the total alkali metal content is strikingly close to $A_{12}Tt_{22}$ and $A_{16}Tt_{31}$ proposed previously from TG/DT analysis data and believed to contain Tt_4^{4-} tetrahedra and Tt_9^{4-} monocapped square antiprisms in ratios 1:2 and 1:3, respectively.[26] In this sense, therefore, it is not unlikely that these preliminary thermogravimetry data might have indicated compositions other than $A_{12}Tt_{22}$ and $A_{16}Tt_{31}$.

$Rb_5Na_3Sn_{25}$. This chiral clathrate was initially identified as a second phase in the product from reaction of Rb, Na, and Sn that was intended to produce $Rb_3Na_{10}Sn_{23}$. It was later synthesized in higher yields but always contained tin as a second phase. There are six tin and three cation positions in the structure. The framework part of the structure and the cations inside the dodecahedra of tin were refined essentially identically as those in $K_{7.4(1)}Sn_{25}$ and K_6Sn_{25}.[13,15] Nevertheless, the positioning of the other two alkali metal sites is different (Figure 8). The two reports on K_xSn_{25} disagree on the range of stoichiometries; i.e., in one, x is given to vary from 7.5 to 8.5 with the accompanying lattice parameter from $a = 16.278(3)$ to $a = 16.461(3)$ Å, and in the other one, x is supposedly fixed at 6 and a is 16.202(2) Å. The nonstoichiometry in the former is the result of one fractionally occupied potassium site, K3, refined in $K_{7.4(1)}Sn_{25}$ with 73% occupancy. Note that occupancy of more than 50% results automatically in impossibly short K3−

(22) Vaughey, J. T.; Corbett, J. D. *Inorg. Chem.* **1997**, *36*, 4316.
(23) Fässler, T. F.; Kronseder, C. *Angew. Chem., Int. Ed. Engl.* **1998**, *37*, 1571.
(24) Volk, K.; Müller, W. *Z. Naturforsch.* **1978**, *33b*, 823.
(25) Müller, W.; Volk, K. *Z. Naturforsch.* **1978**, *33b*, 275.
(26) von Schnering, H.-G.; Baitinger, M.; Bolle, U.; Carrilo-Cabrera, W.; Curda, J.; Grin, Y.; Heinemann, F.; Llanos, J.; Peters, K.; Schmeding, A.; Somer, M. *Z. Anorg. Allg. Chem.* **1997**, *623*, 1037.

Table 4. Important Distances (Å) in $Rb_5Na_3Sn_{25}$

bond			bond		
Sn1−	3Sn2	2.858(1)	Rb1−	3Sn4	3.817(1)
	3Na3	3.49(2)		Sn6	3.845(2)
	3Rb2	3.742(5)		3Sn3	3.913(1)
	Rb1	4.415(2)		3Sn2	3.914(2)
	3Rb2	4.434(6)		3Sn2	3.990(1)
Sn2−	2Sn4	2.827(1)		3Sn4	4.033(1)
	Sn1	2.858(1)		3Sn5	4.222(2)
	Sn2	2.865(1)		Sn1	4.415(2)
	Rb1	3.914(2)	Rb2−	Sn5	3.646(4)
	Rb1	3.990(1)		Sn1	3.742(5)
	Rb2	3.999(4)		Na3	3.62(2)
	Rb2	4.050(4)		Sn4	3.856(5)
	Rb2	4.489(5)		Sn5	3.904(5)
	Rb2	4.538(5)		Sn4	3.922(4)
Sn3−	2Sn5	2.871(1)		Sn2	3.999(4)
	2Sn4	2.874(1)		Sn5	4.028(6)
	Na3	3.68(2)		Sn3	4.032(5)
	2Rb1	3.913(1)		Sn2	4.050(4)
	2Rb2	4.032(5)		Sn2	4.378(6)
Sn4−	2Sn2	2.827(1)		Sn6	4.429(4)
	Sn3	2.874(1)		Sn1	4.434(6)
	Sn5	2.875(1)		Sn2	4.489(5)
	Rb1	3.817(1)		Sn4	4.527(5)
	Rb2	3.856(5)		Sn2	4.538(5)
	Rb2	3.922(4)		Na3	4.76(2)
	Rb1	4.033(1)		Na3	4.90(2)
	Rb2	4.527(5)		Sn4	5.074(6)
	Rb2	5.074(6)		Na3	5.37(2)
Sn5−	Sn3	2.871(1)		Sn3	5.456(6)
	Sn4	2.875(1)		Na3	5.48(2)
	Sn6	2.8780(9)		Sn5	5.544(5)
	Na3	3.07(2)		Sn5	5.693(7)
	Na3	3.10(2)	Na3−	Sn5	3.07(2)
	Na3	3.41(2)		Sn5	3.10(2)
	Rb2	3.646(4)		2Na3	3.19(2)
	Rb2	3.904(5)		Sn5	3.41(2)
	Rb2	4.028(6)		Sn1	3.49(2)
	Rb1	4.222(2)		Rb2	3.62(2)
	Rb2	4.378(6)		2Na3	3.63(4)
Sn6−	Sn6	2.849(2)		Sn3	3.68(2)
	3Sn5	2.8780(9)		Sn4	4.42(2)
	Rb1	3.845(2)		Sn6	4.70(1)
	3Rb2	4.429(4)		Sn2	4.75(2)
	Sn6	4.708(4)			
	Sn6	4.708(4)			

K3 contacts of 2.92 Å and also that the electronically balanced stoichiometry A_8Sn_{25} corresponds to an occupancy of 83.3%.

An important feature in $Rb_5Na_3Sn_{25}$ is that not all tin atoms are four-bonded, just as in the structures of $A_3Na_{20}Sn_{23}$. Two positions, Sn1 and Sn5, that account for 8 out of the 25 tin atoms are 3-bonded and carry a formal charge of −1, i.e., Sn^-. An electronically balanced compound would have stoichiometry A_8Tt_{25}, and therefore, both K_6Sn_{25} and $K_{7.4}Sn_{25}$ are electron-deficient. The stoichiometry of the former has been rationalized as emptying some lone-pair orbitals on the three-bonded tin atoms as a result of repulsive interactions with each other.[27] The ternary analogues $K_6Sn_{23}Bi_2$ and $Ba_6In_4Ge_{21}$ [14,15] and the binary-phase Ba_6Ge_{25},[16] on the other hand, are electronically balanced and electron-rich compounds, respectively, with apparently no repulsion between the same lone pairs.

The cations in $K_6Sn_{23}Bi_2$ (a = 16.300(2) Å) were refined at different positions than in $K_{7.4(1)}Sn_{25}$. The general position K3 in the latter is a special position on a 2-fold axis in the former and results in fewer cations. In $Rb_5Na_3Sn_{25}$ the site corresponding to the K3 site is a general position labeled Rb2, which is refined as 50% occupied because it is close to its equivalent generated by the very close 2-fold axis. Furthermore, the equivalent to the special position K2 in $K_{7.4}Sn_{25}$ is also made general, labeled Na3, and refined as 50% occupied. Thus, Na3 and Rb2 account for one full cation. We do not find any electron density at the special site corresponding to K2 or at the special position for K3 in $K_6Sn_{23}Bi_2$.

Shown in Figure 8a are the locations of Rb2 and Na3, which reside between the helical chains of face-sharing dodecahedra of tin. They are surrounded by 20 tin atoms that form incomplete tetrakaidecahedron. The Na3 position is near the square of Sn1−Sn5−Sn5−Sn5, the open side of this incomplete polyhedron (Figure 8b). The coordination around Na3 is made of eight Sn and five cations at distances ranging from 3.07(2) to 4.75(2) Å and from 3.19(1) to 3.63(4), respectively. The multiplicity of this general position is 6 times that of the special position of K2 refined in $K_{7.4(1)}Sn_{25}$. The distance from Na3 to Rb2 becomes unreasonably short of ca. 2 Å, and this and the fact that Rb2 is 50% occupied suggested the same occupation for Na3 and therefore ideal composition of A_8Sn_{25}. The thermal parameters for both Rb2 and Na3 remained relatively large and quite anisotropic, elongated in one direction. It is almost as if the electron density within the space enclosed between the chiral chains is nearly continuous. Similar effects of "smeared" electron density and fractional occupancy of the cation sites are often observed in tunnel-like structures with large cations. It is not difficult to understand the "displacement" of the alkali metal cations from the center of the oversized cavity, often referred to as "rattling" motion.

The lattice parameters of $Rb_5Na_3Sn_{25}$ are independent of the loaded stoichiometries and are quite similar to those of K_xSn_{25} with x = 8,[13] i.e., the composition near the ideal stoichiometry (a = 16.4127(7) vs a = 16.392(8) Å, respectively). The stoichiometry corresponding to the electronically balanced compound, $Rb_5Na_3Sn_{25}$, is supported by the magnetic susceptibility measurements, temperature-independent diamagnetic behavior characteristic of saltlike Zintl compounds.

In conclusion, the importance of available cations with very different sizes should be stressed again. The compounds described here as well as those of stoichiometric Si- and Ge-based clathrate-II are possible only with such mixed alkali metals. We have now expanded these studies into the smallest alkali metal, lithium, and have found even more unexpected results such as isolated arachno clusters of $[Sn_8]^{6-}$ and closo clusters of $[Ge_{12}Li_4]^{8-}$.[28,29]

Acknowledgment. We thank the Donors of the Petroleum Research Fund administered by the ACS for support of this research and the NSF for an equipment grant (DMR-9703732) for the SQUID magnetometer.

Supporting Information Available: An X-ray crystallographic file, in CIF format, for the four structures and tables listing interatomic distances and atomic positional parameters for $Rb_3Na_{10}Sn_{23}$ and $K_3Na_{10}Sn_{23}$. This material is available free of charge via the Internet at http://pubs.acs.org.

IC0007714

(27) Fässler, T. F. *Z. Anorg. Allg. Chem.* **1998**, *624*, 569.

(28) Bobev, S.; Sevov, S. C. *Angew. Chem.*, in press.

(29) Bobev, S.; Sevov, S. C. Unpublished research.